HYBRIDGE

Distributed Control and Stochastic Analysis of Hybrid Systems
Supporting Safety Critical Real-Time Systems Design

WP1: Identification and modelling of uncertain hybrid systems

Simplified Multi-Aircraft Models for Conflict Detection and Resolution Algorithms

W. Glover[1] and J. Lygeros[2]

Sep 30, 2004

Version:*1.1*
Task number:*1.4*
Deliverable number:*D1.4*
Contract:*IST-2001-32460 of European Commission*

[1] Department of Engineering, University of Cambridge, U.K.
[2] Department of Electrical and Computer Engineering, University of Patras, Greece.

DOCUMENT CONTROL SHEET

Title of document:	*A multi-aircraft model for conflict detection and resolution algorithm evaluation*
Authors of document:	*W. Glover and J. Lygeros*
Deliverable number:	*D1.4*
Contract:	*IST-2001-32460 of European Comission*
Project:	*Distributed Control and Stochastic Analysis of Hybrid Systems Supporting Safety Critical Real-Time Systems Design (HYBRIDGE)*

DOCUMENT CHANGE LOG

Version #	Issue Date	Sections affected	Relevant information
0.1	18/12/2003	All	First draft
0.2	6/1/2004	All	Second draft
1.0	9/6/2004	All	Submitted to the consortium
1.1	28/8/2004	All	Revised based on reviewers comments
1.2	30/9/2004	All	Revised based on reviewers comments

Version 1.2		Organisation	Signature/Date
Authors	W. Glover	UCAM	
	J. Lygeros	U. Patras	
Internal reviewers	H. Blom	NLR	
	R. Irvine	EEC	
	M. Prandini	UniBs	

HYBRIDGE, IST-2001-32460
Work Package WP1, Deliverable D1.4

Simplified Multi-Aircraft Models for Conflict Detection and Resolution Algorithms

Prepared by:
W. Glover* and J. Lygeros†

Abstract

Simplified models used in conflict detection and resolution are presented. When simplifying the models that do not significantly affect their capability of predicting dangerous encounters Analysis is performed to determine how accurate these models are and what assumptions can be made when simplifying the models that do not significantly affect their capability of predicting dangerous encounters. Extensive simulations are performed to analyze the effect of wind correlation on conflict probability.

*Department of Engineering, University of Cambridge, Cambridge, CB2 1PZ, UK, Tel. +44122333260, Fax. +441223332662, wg214@eng.cam.ac.uk

†Department of Electrical and Computer Engineering, University of Patras, Rio, Patras, GR-26500, GREECE, Tel. +30 2610 996 458, Fax. +30 2610 991 812, lygeros@ee.upatras.gr

Contents

List of Figures

List of Tables

1 Aim and Scope

The main aim of Deliverable D1.4 of HYBRIDGE is summarized in Task 1.4 of WP1:

> Deduce simplified models, on which conflict prediction and resolution algorithms can be based. Model reduction will strike a balance between on the one hand tractability and computational efficiency and on the other accuracy and validity. Different models will be developed for different conflict detection and resolution approaches. The process will be iterative: the models will be tuned until the performance of the algorithms based on them is deemed acceptable.

The model developed in WP1 documented in deliverable D1.3 [7] was based on a number of simplifying assumptions:

1. Spoilers, flaps, etc. are not used as inputs. Their effect on the aerodynamic parameters is considered.
2. The angle of attack and side-slip angles are small. The flight path angle and the bank angle are treated as inputs rather than states.
3. Ground speed is given by a simple addition of wind speed to airspeed.
4. A 3D Flight Management System (FMS) is used. Aircraft do not correct for along track errors.
5. During final approach and landing, no attempt is made to track a glide path. As a consequence the aircraft generally tend to miss the beginning of the runway longitudinally.
6. The same controller is used to track straight paths and turns.
7. No nominal weather data is provided to the model. The nominal wind is zero and all wind is treated as a stochastic perturbation.
8. Aircraft turning at a way point ignore the measured wind and compute the point where they should start their turn as though the wind was zero.
9. The model ignores the effect of weather phenomena other than wind speed (e.g. fluctuations in humidity).
10. The model described in D1.3 assumes all aircraft have the same FMS. i.e. All aircraft have the same deviation statistics whereas in fact some aircraft (those with lateral FMS) will perform very well whereas others (Human piloted aircraft) will perform much worse.

The model also contains a number of complications introduced to make it more realistic, which make it more difficult to deal with from a computational point of view. The most prominent are:

1. A detailed model of the wind field and its correlation structure.
2. A detailed model of the lateral corrective action of the FMS.
3. A detailed model of the discrete dynamics of the FMS.
4. Nonlinear continuous dynamics.

The issues listed first are the ones that are the most demanding computationally.

In D1.4 we discuss a number of improvements that have been pursued to resolve some of the outstanding issues listed above and make the model presented in D1.3 more accurate (Section 2). We also discuss a number of simplifications that can be introduced to make the model more usable for conflict detection and resolution purposes (Section 3). Finally, we discuss a number of simplified models that have been used in HYBRDIGE and the literature to perform predictions to be used for probabilistic conflict detection and resolution (Section 4) and highlight the simplifications each of them makes.

2 Improvements to the model of D1.3

2.1 The 3D FMS assumption

In this section we address the simplifying assumption listed in item 4 of Section 1. In D1.3 we assumed a 3D FMS system which is the system commonly used currently. There are two alternative FMS systems: 4D and 3.5D. 4D FMS involves the calculation of a 4D trajectory before take-off which the aircraft must follow. This has the effect of producing less optimal (in terms of fuel consumption) but more predictable trajectories. 3.5D is less constrictive than 4D. The aircraft are constrained to reach certain points at certain times, for example ensure that an aircraft arrives at its destination airport on schedule. 3.5D as its name suggests is half way between 3D and 4D in terms of predictability and optimality. For a discussion of the issues and possible designs of 3.5D and 4D FMS the reader is referred to [1]. 4D FMS is probably less interesting from the point of view of conflict detection due to the fact that 4D trajectories are more predictable and hence conflicts become more predictable and probabilistic methods are less useful. It will still be interesting from the point of view of accident risk modelling which deals with much rarer occurrences. 3.5D FMS will still be interesting in the early stages of flight were there are still large uncertainties but less interesting in later stages where the flight becomes more constrained. Due to the above points and since 3D FMS is the current standard in the industry 3.5D and 4D FMS are beyond the scope of this work package and hence we have only implemented 3D FMS.

2.2 Introduction of nominal wind

In this section we address the simplifying assumption listed in item 7 of Section 1. In D1.3 we performed analysis of wind data to produce statistic for the correlation of the wind as a function of spatial, temporal and altitude difference. A drawback of this method is that it only gives statistics for the nominal wind. In reality air traffic controllers have some weather prediction information available to them so the variance and correlation in the stochastic term of the wind would be much smaller. To alleviate this problem we have found two new sources of data, [16] and [11]. [16] uses the difference between predicted winds and measured wind to produce their statistics. [11] uses the difference between average ground speed and actual ground speed. The correlation distances in [16] are smaller than in [7] but only by roughly a factor of two, suggesting that our approximation was satisfactory. The correlation in time also has the same harmonic structure as in [7]. This is reflected by a periodic term in the correlation function (see Table 3). The harmonic signal is likely due to the diurnal cycle. The correlation in [11] is much smaller but this is probably due to the fact that the ground speed is averaged only over a time period of roughly 20 minutes. Both of these documents neglected high frequency wind

variable	u	v
a	0.75	0.91
b (km)	311	363
c	0.05	-0.06
f(0)	0.80	0.85

Table 1: Fit parameters for Error Correlation vs. Horizontal Separation from [16]. Correlation function is: $f(x) = (a \exp(-x/b) + c$

variable	u	v
a	0.96	1.25
b (mb)	153	273
c	-0.16	-.041
f(0)	0.81	0.84

Table 2: Fit parameters for Error Correlation vs. Pressure Separation from [16]. Correlation function is: $f(x) = a \exp(-x/b) + c$. At cruise altitudes 1mb is roughly 24 metres.
.

such as turbulence that have minimal effect on the positional uncertainty of the aircraft. The results from [16] are presented in Tables 1, 2 and 3. The results show the correlation in both the easterly (u) and northerly (v) components of the wind.

In light of the results from [16] we have updated the correlation function that is now implemented in the simulator as:

$$\rho_{xy}(t, P, t', P') = \sigma(z)\sigma(z') \exp\left(-\lambda|t - t'|\right) \exp\left(-\beta \left| \begin{array}{c} x - x' \\ y - y' \end{array} \right|\right) \exp\left(-\gamma|z - z'|\right) \quad (1)$$

where $\lambda = 6e-6s^{-1}$, $\beta = 1.6e-6m^{-1}$, $\sigma(z) = 7.7ms^{-1}$. The correlation function is similar to the results of [16] but we have neglected the harmonic component in the temporal separation since it is only observed at a very large scale. We have also made the function isotropic so the correlation is the same in all directions.

For this report we have not extracted values for γ since all of our tests have been for level flights. We will do this to code the landing problem for WP5.

2.3 Improvements to the turn model

In this section we address the simplifying assumption listed in item 8 of Section 1.

Under this simplifying assumption the algorithm for calculating when the aircraft should turn does not take into account the wind velocity. This leads to overshoots when there

variable	RUC u	RUC v
a	0.70	0.86
b (minutes)	141	254
c	0.14	0.10
d	0.06	0.05
e (minutes)	97	447
f (minutes)	1275	935
f(0)	0.90	0.91

Table 3: Fit parameters for Error Correlation vs. Temporal Separation from [16]. Correlation function is: $f(x) = a\exp(-x/b) + c + d\cos(2\pi(x-e)/f)$

is a strong tail wind. Modern aircraft FMS do take the wind into account and if the simulator is to reflect the state of current aircraft performance the simulator should be able to simulate this. One method for doing this is described below.

2.3.1 Notation

First of all we introduce some notation:

$O(i)$	Coordinates of way point i (from CFMU, $O(i) \in \mathbb{R}^3$)
$\Psi(i)$	Angle i^{th} segment of nominal path makes with $X-$axis (computed from $O(i)$)
$\Psi_h(i,w)$	Nominal heading of aircraft (relative to air) for i^{th} segment of flight plan.
Ψ_w	Angle of wind vector
v	Velocity vector of aircraft relative to air
w	Wind vector
v_g	Velocity of aircraft relative to the ground
r	distance from aircraft to the center of the turn

2.3.2 Straight Flight

First of all we describe how the aircraft should track a straight path when it has knowledge of the wind velocity. Figure 1 shows the relationship between the air velocity, wind velocity and the ground velocity. We wish to control the heading of the aircraft so that the ground velocity is parallel with the reference course. Using the sine rule we can deduce that the aircraft needs to select its heading according to

$$\Psi_h(i,w) = \Psi(i) - sin^{-1}\left(\frac{||w||\sin(\Psi_w - \Psi(i))}{v}\right) \tag{2}$$

where $\Psi(i)$ is the angle of the ground speed with respect to the x-axis of the global

coordinate frame, $\Psi_h(i, w)$ is the heading of the aircraft, θ_w is the angle of the wind velocity and v is the airspeed of the aircraft.

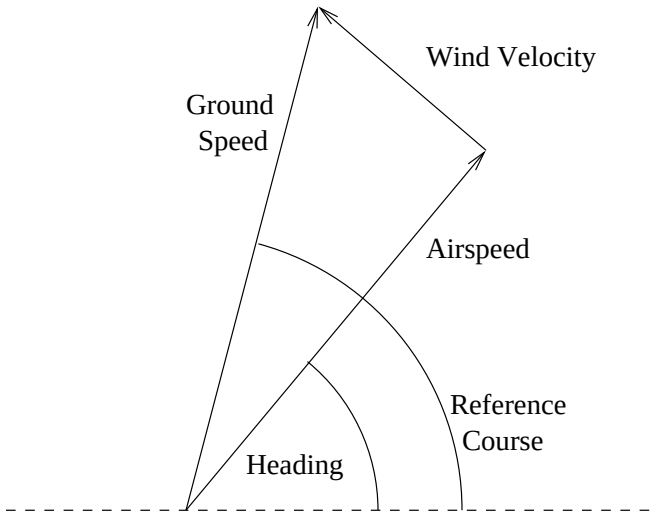

Figure 1: Diagram showing the wind triangle used to calculate heading from reference course and wind speed.

2.3.3 Turns

Consider an aircraft executing a turn at way point $O(i+1)$, i.e. switches from reaching the straight line segment $O(i+1)-O(i)$ to tracking the straight line segment $O(i+2)-O(i+1)$. As in D1.3 we define $\Psi(i) = \tan^{-1}\left(\frac{y(i+1)-y(i)}{x(i+1)-x(i)}\right)$.. For the following we will assume that when calculating the start point of a turn the FMS assumes that throughout the turn the aircraft will maintain a constant airspeed and altitude and that the wind velocity will be constant. Using part 2.3.2 we can calculate the heading needed to track the straight line segments before and after the turn. We wish to calculate a turn such that the aircraft ends the turn on the next segment with the correct heading. Using the assumption of constant airspeed and bank angle we can compute the time taken for the turn and a vector representing the distance travelled through the air during the turn.

$$\Psi_{hd} = \Psi_h(i+1, w) - \Psi_h(i, w) \tag{3}$$

$$\Psi_{hs} = sign(\Psi_{hd}) \tag{4}$$

$$t_{\text{turn}} = \frac{v\Psi_{hd}\Psi_{hs}}{g\tan(\phi_{nom})} \tag{5}$$

Where Ψ_{hd} denotes the difference between the heading before the turn and the heading after the turn, Ψ_{hs} denotes the direction of the turn and t_{turn} is the time taken to complete

the turn. Using the time taken we can compute the displacement of the aircraft due to the wind.

$$w_{turn} = t_{\text{turn}} w \tag{6}$$

By addition of this to the nominal movement of the aircraft we get the change in position of the aircraft during the turn.

$$c = \frac{v}{g\tan(\phi_{nom})}\left(w\Psi_{hs}\Psi_{hd} + v\begin{bmatrix}\cos\left(\Psi_h(2) - \frac{\pi}{2}\Psi_{hs}\right) - \cos\left(\Psi_h(1) - \frac{\pi}{2}\phi_{hs}\right)\\ \sin\left(\Psi_h(2) - \frac{\pi}{2}\Psi_{hs}\right) - \sin\left(\Psi_h(1) - \frac{\pi}{2}\phi_{hs}\right)\end{bmatrix}\right) \tag{7}$$

The geometry of the situation is depicted in Figure 2. The vector c will be the same as the vector from the start of the turn to the waypoint O_i plus the vector from the waypoint to the end of the turn. Now consider the vector c as a linear combination of the unit vector parallel to $\overrightarrow{O_iO_{i+1}}$ and the unit vector parallel to $\overrightarrow{O_{i+1}O_{i+2}}$. The first component of this vector will tell us the the distance before the waypoint on the first segment at which the aircraft should begin its turn.

$$d = \left[\frac{O(i+1) - O(i)}{||O(i+2) - O(i+1)||}, \frac{O(i+1) - O(i+1)}{||O(i+2) - O(i+1)||}\right]^{-1} c \tag{8}$$

2.3.4 Constant ground radius turns

The alternative to constant bank angle turns are constant ground radius turns. Constant ground radius turns are used by modern FMS when an aircraft tracks a reference circular pattern which is fixed relative to the ground. This will involve a changing bank angle in the presence of wind.

We will now show how to compute the bank angle necessary to track a circular arc of radius r with respect to the ground in the presence of wind w.

Using the sine rule:

$$\sin(\Psi_c - \Psi_h) = \frac{\sin(Psi_w - \Psi_c)||w||}{||v||}$$

Taking derivatives:

$$\frac{d\Psi_h}{dt} = \frac{d\Psi_c}{dt}\frac{\cos(\Psi_w - \Psi_c)||w||}{\cos(\Psi_c - \Psi_h)||v||} + \frac{d\Psi_c}{dt}$$

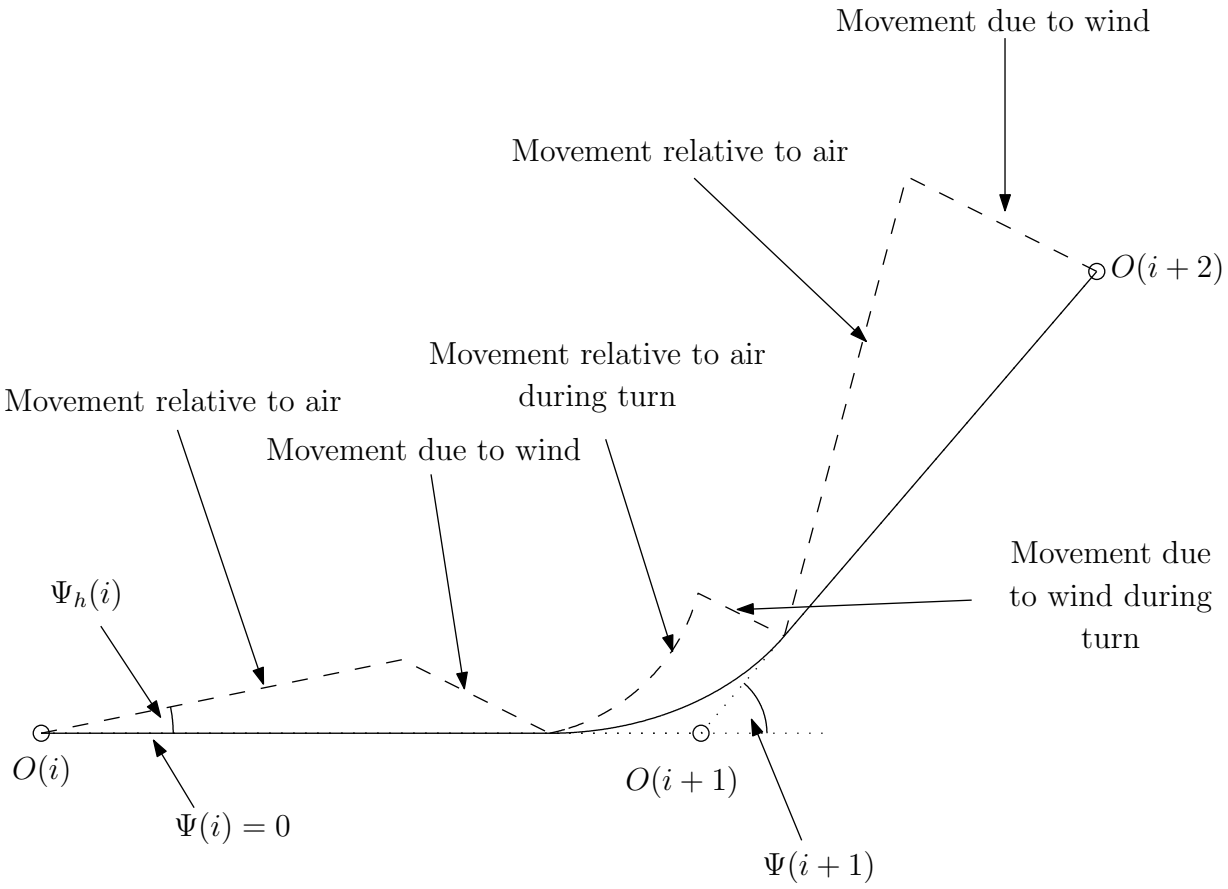

Figure 2: Diagram showing turn in wind.

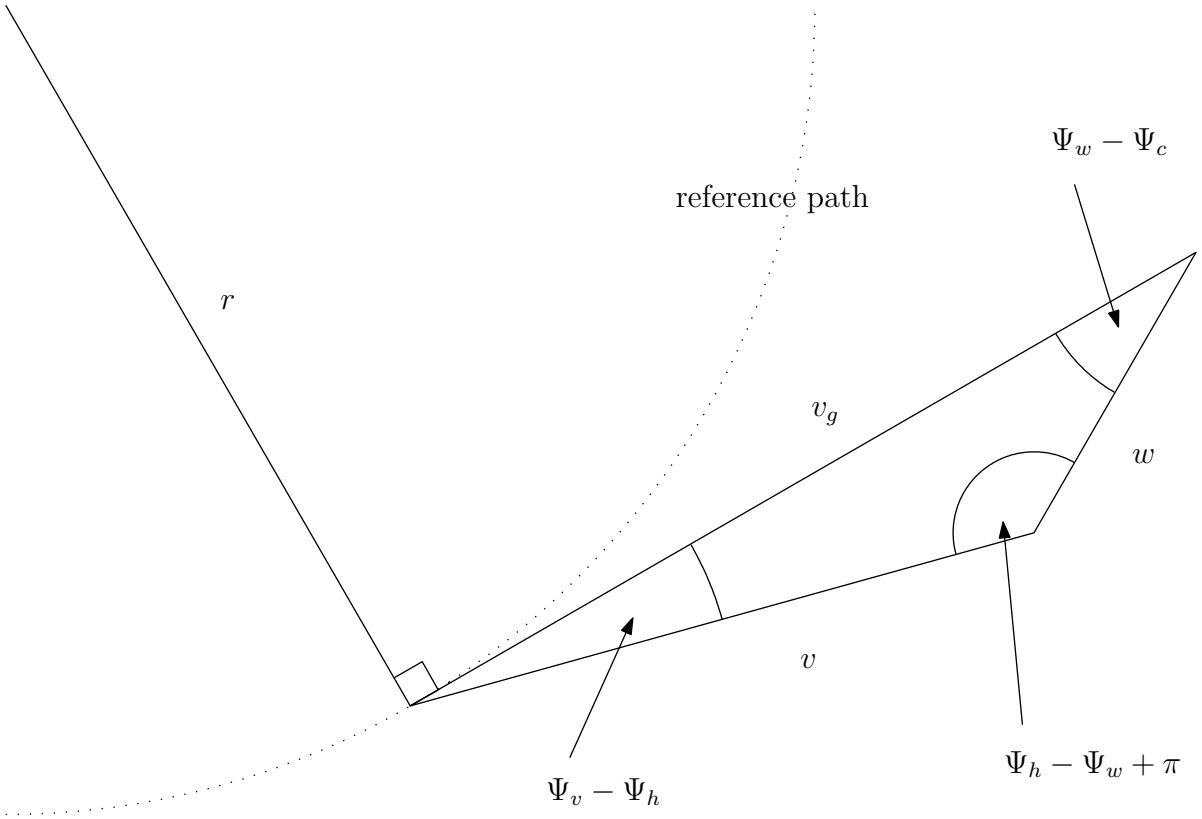

Figure 3: Diagram showing constant ground radius turn

$$= \frac{d\Psi_c}{dt}\left(\frac{\cos(\Psi_w - \Psi_c)||w||}{\cos(\Psi_c - \Psi_h)||v||} + 1\right)$$
$$\frac{d\Psi_c}{dt} = \frac{v_g}{r}$$

Using the sine rule once more:

$$\frac{d\Psi_c}{dt} = \frac{\sin(\Psi_w - \Psi_h)||v||}{\sin(\Psi_w - \Psi_c)r}$$

Finally:

$$\frac{d\Psi_h}{dt} = \frac{\sin(\Psi_w - \Psi_h)||v||}{\sin(\Psi_w - \Psi_c)r}\left(\frac{\cos(\Psi_w - \Psi_c)||w||}{\cos(\Psi_c - \Psi_h)||v||} + 1\right)$$
$$\phi = \sin^{-1}\left(\frac{2x_6\sin(\Psi_w - \Psi_h)||v||}{C_L S_\rho \sin(\Psi_w - \Psi_c)r}\left(\frac{\cos(\Psi_w - \Psi_c)||w||}{\cos(\Psi_c - \Psi_h)||v||} + 1\right)\right)$$

2.4 Nominal flight path for final approach

In this section we will the simplifying assumption from item 5 of section 1. This is beyond the scope we had originally envisioned for the model, which was originally intended to provide support for en-route conflict detection and resolution. However recent work under WP5 could also provide a methodology to address the problem of selecting approach and holding patterns and sequencing aircraft for landing. To support this effort we provide rudimentary controllers for final approach. We will model the approach of the aircraft from the final penultimate to the beginning of the runway. We will use the same simplifications as with the rest of the model, so we will model the descent but will not model the flare out at the bottom of the descent. Recall that the, though not used explicitly as inputs the effect of spoilers, flaps etc. on lift and drag is still considered. With the model from [7] the aircraft would tend to miss the beginning of the runway. This was because the thrust was fixed and flight path angle was used to control speed. To resolve this problem we will choose the controls to force the aircraft to follow a straight line from the penultimate waypoint to the runway. This will be achieved by essentially fixing the flight path angle and using the thrust to control the airspeed.

We rearrange the total energy equation which is used in [6] to find the required amount of thrust in terms of the desired descent rate and the desired energy share factor. The total energy share factor is calculated in the same way as in [7].

$$\frac{dh}{dt} = \left[\frac{(T-D)V_{TAS}}{mg}\right] f(M) \implies T = \frac{dh}{dt}\frac{mg}{V_{TAS}f(M)} + D \tag{9}$$

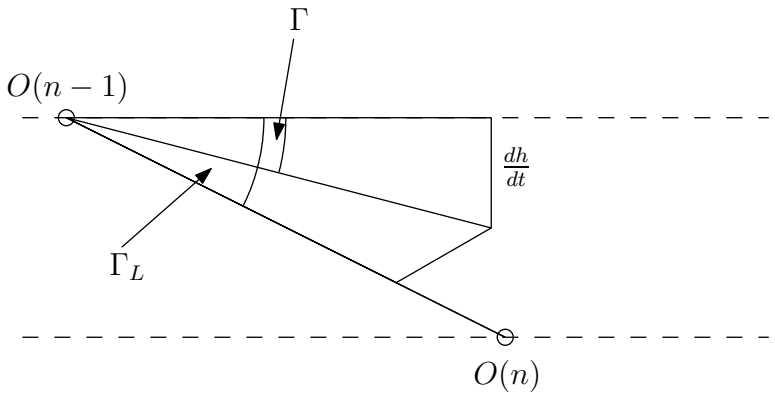

Figure 4: Final descent

Figure 4 shows how the required descent rate is calculated in the presence of wind. The figure shows the vertical plane as the aircraft approaches the runway. Here Γ_w is the angle of the wind in the vertical plane, Γ is the flight path angle of the aircraft, $\frac{dh}{dt}$ is the descent rate, $O(n-1)$ is the penultimate waypoint and $O(n)$ is the final waypoint at the beginning of the runway. The required descent rate can easily be computed by using the sine rule:

$$\frac{||w||}{\sin(\Gamma_L - \Gamma)} = \frac{||v||}{\sin(\Gamma_w - \Gamma_L)} \implies \Gamma = \Gamma(n-1) - \sin^{-1}\left(w \sin(\Gamma_w - \Gamma(n-1))||v||\right) \tag{10}$$

$$\implies \frac{dh}{dt} = \Gamma_L - \sin^{-1}\left(\frac{||w||}{||v||}\sin(\Gamma_w - \Gamma_L)\right) \tag{11}$$

Substituting this back into equation (9) we get:

$$T = \left[\Gamma_L - \sin^{-1}\left(\frac{||w||}{||v||}\sin(\Gamma_w - \Gamma_L)\right)\right]\frac{mg}{||v||f(M)} + D \tag{12}$$

2.5 An improvement in the computational implementation for wind correlation

In [7] we presented an algorithm for synthesising a wind field with a given correlation structure. We have since improved the efficiency of the method and made it more general.

Recall that the stochastic wind component is modelled as a random field:

$$w : \mathbb{R} \times \mathbb{R}^3 \to \mathbb{R}^3$$

where $w(t,x)$ represents the wind at point $x \in \mathbb{R}^3$ at time t.

We assume that the wind field is jointly gaussian. For simulation purposes we wish to find a method where we can extract a gaussian random variable which has a known correlation to other jointly gaussian variables which have already been calculated. For this we need the following to ensure that for any $t_1, \ldots, t_n$, $x_1, \ldots, x_n$ The corresponding correlation matrix

$$\begin{pmatrix} E(w(t_1,x_1)w(t_1,x_1)) & \ldots & E(w(t_1,x_1)w(t_n,x_n)) \\ \vdots & & \vdots \\ E(w(t_n,x_n)w(t_1,x_1)) & \ldots & E(w(t_n,x_n)w(t_n,x_n)) \end{pmatrix} \tag{13}$$

is symmetric positive definite. To simplify the notation we will denote $w_i = w(t_i, x_i)$, $m_i = E(w_i)$ and $\rho_{ij} = E[(w_i - m_i)(w_j - m_j)]$.

To start the process we simply extract $w_1 \sim N(m_1, \rho_{11})$. At step n of the simulation, suppose we have already extracted n jointly gaussian random variables

$$\begin{pmatrix} w_1 \\ \vdots \\ w_n \end{pmatrix} \sim N\left[\begin{pmatrix} m_1 \\ \vdots \\ m_n \end{pmatrix}, \begin{pmatrix} \rho_{11} & \ldots & \rho_{1n} \\ \vdots & & \vdots \\ \rho_{1n} & \ldots & \rho_{nn} \end{pmatrix} \right] \tag{14}$$

Suppose also we have lower triangular$\{B_{ij}\}$ so that we can compute w_i by:

$$\begin{pmatrix} w_1 \\ \vdots \\ w_n \end{pmatrix} = \begin{pmatrix} B_{11} & & 0 \\ \vdots & \ddots & \\ B_{n1} & \ldots & B_{nn} \end{pmatrix} \begin{pmatrix} g_1 \\ \vdots \\ g_n \end{pmatrix} + \begin{pmatrix} m_1 \\ \vdots \\ m_n \end{pmatrix} \tag{15}$$

We wish to compute w_{n+1} so that

$$\begin{pmatrix} w_1 \\ \vdots \\ w_n \\ w_{n+1} \end{pmatrix} \sim N\left[\begin{pmatrix} m_1 \\ \vdots \\ m_n \\ m_{n+1} \end{pmatrix}, \begin{pmatrix} \rho_{11} & \ldots & \rho_{1n} & \rho_{1(n+1)} \\ \vdots & & \vdots & \vdots \\ \rho_{1n} & \ldots & \rho_{nn} & \rho_{n(n+1)} \\ \rho_{1(n+1)} & \ldots & \rho_{(n+1)n} & \rho_{(n+1)(n+1)} \end{pmatrix} \right] \tag{16}$$

If we could find $B_{n+1,0}, \ldots, B_{n+1,n+1}$ such that:

$$\begin{pmatrix} w_1 \\ \vdots \\ w_n \\ w_{n+1} \end{pmatrix} = \begin{pmatrix} B_{11} & 0 & \ldots & 0 \\ \vdots & \ddots & \ddots & \vdots \\ B_{n1} & \ldots & B_{nn} & 0 \\ B_{(n+1)1} & \ldots & B_{(n+1)n} & B_{(n+1)(n+1)} \end{pmatrix} \begin{pmatrix} g_1 \\ \vdots \\ g_n \\ g_{n+1} \end{pmatrix} + \begin{pmatrix} m_1 \\ \vdots \\ m_n \\ m_{n+1} \end{pmatrix} \tag{17}$$

Then the computation of w_{n+1} will be straight forward, since g_{n+1} is gaussian, zero mean, variance 1 and can be extracted independently of everything else.

$$\{\rho_{ij}\} = E\left[(w_i - m_i)(w_i - m_i)^T \right] \;=\; E\left[B_{ij} g_i g_i^T B_{ij}^T \right] \tag{18}$$

$$= B_{ij} E\left[g_i g_i^T\right] B_{ij}^T \quad (19)$$
$$= B_{ij} B_{ij}^T \quad (20)$$

By equating coefficients on both sides we find:

$$B_{k,i} = \left[\rho_{k,i} - \sum_{l=0}^{i-1} B_{k,l} B_{i,l}\right] (B_{i,i})^{-1} \quad (21)$$

$$B_{ii} = \sqrt{\rho_{ii} - \sum_{k=1}^{i-1} B_{ik}^2} \quad (22)$$

Because the correlation matrix is symmetric positive definite, the expression under the square root is always positive, and all B_{ij} are real.

It should be noted that this algorithm is essentially the same as the Cholesky decomposition of the matrix. The main difference is that it needs to be applied one row at a time, since the correlation depends on the positions of the aircraft which in turn depends on the wind strength at previous times. The processing time for this algorithm varies with the cube of the number of values needed.

2.6 Other improvements that can be pursued

We have described extensions to some of the assumptions listed in Section 2. The remaining assumptions are generally considered in the literature to have a small relative impact on aircraft trajectories and can hence be ignored.

For example weather uncertainty other than wind speed, such as temperature and humidity have been shown in the literature to have a much smaller relative effect on aircraft trajectories, so they can safely be ignored [8].

3 Simplifications and their impact on model accuracy

3.1 Ignore the wind correlation

In this section we will study the impact of ignoring wind correlation on the ability of the model to predict future conflict. Modelling wind correlation produces two effects:

- Correlation in the disturbances experienced between aircraft. For example an if two aircraft are close together and facing the same direction and one experiences a head wind then the other is likely to experience a similar head wind. This effect is neglected in most conflict detection algorithms.
- Correlation in the disturbances that a single aircraft experiences at different times. For example, if an aircraft is travelling in a straight line the wind it experiences is likely to change gradually. Most conflict detection algorithms consider this disturbance to be white noise [15] or they consider it to be constant during the period of the encounter [13].

For our comparison we will neglect cross-track error. In reality there will be some cross-track error but cross-track error is hard to quantify accurately since in reality it is caused by the effect of numerous factors, not just the wind. Also cross-track errors tend to be small in modern aircraft (see Section 3.3) and will become smaller as technology advances. Figure 6 shows that the effect of cross-track error is relatively small.

We will consider two different methods for estimating the conflict probability:

- Monte Carlo simulation using the simulator with lateral perturbations ignored. For this estimate conflict probability by performing 1,000 simulations and finding what fraction enter conflict.
- Modified conflict probe from [13]. We use the same conflict probe except with the lateral perturbations ignored. The effect of ignoring lateral perturbations can be seen in Figure 6. We also modify the conflict probe so that correlation in the wind can be taken into account.

For the simulations we will consider both the full simulation and also simulations where the wind is assumed to be constant for each aircraft.

Due to the large number of parameters available for two aircraft encounters we will only consider level flight where the minimum predicted separation is zero. We will consider three different crossing angles (45°, 90°, 135°) and six different values for expected time until minimum separation (5,10,15,20,25,30).

The results are presented in figure 5. Plots in the left column corresponds to simulations without correlation between aircraft. Plots in the right columns correspond to simulations with correlation between aircraft. In each plot the dotted line represents Monte Carlo simulations with constant wind for each aircraft and the continuous line represents simulations with stochastic wind for each aircraft. The dashed line in the left column represents the Erzberger Paielli conflict probe. The dashed line in the right column corresponds to the Erzberger Paielli conflict probe which has been modified to include wind correlation. The first row corresponds to a crossing angle of 45° the second 90° and the third 135°.

The graphs show that correlation between aircraft has a large impact on conflict probability for the 45° and 135° crossing angles. It has no impact for the 90° crossing angle because the correlation between aircraft for the along track wind speed becomes zero in this case.

The graphs verify that the Erzberger Paielli conflict probe works very well under the assumptions of constant wind, in both the uncorrelated and correlated cases and for all crossing angles. The effect of a non-constant wind has little effect on the conflict probability. This is because the correlation is so high. For aircraft that are cruising and descending the effect will be much greater because the correlation will be much lower. In all cases the non-constant wind causes the conflict probability to be higher. This is because there is more variation in the trajectories during the period of conflict.

The results suggest that for level flight the wind can be assumed to constant over a period of 15-30 minutes. This will greatly increase the speed of Monte Carlo simulations.

3.2 Ignoring the turn model

Many conflict probes ignore turns ([15], [9]) in the interests of tractability. Typically the probe assumes that the aircraft will reach the next way point along a straight track and then turn instantaneously to head for the next way point. This introduces an extra element of uncertainty in the predictions since the total distance covered by the aircraft will be larger than the distance flown by aircraft using a "fly by" FMS (assumed here) and smaller than the distance flown by aircraft using a "fly-over" FMS (discussed briefly in [7]). Figure 8 shows the effect of this in terms of distance for an aircraft at typical cruising speed. It can be seen that for angles less than about 30° the difference is negligible, whereas for angles greater than 90° the difference is significant. If we assume a fly by FMS (which is standard for modern aircraft) the error is always in the same direction, the simplified model will estimate longer paths than the realistic model for all cases.

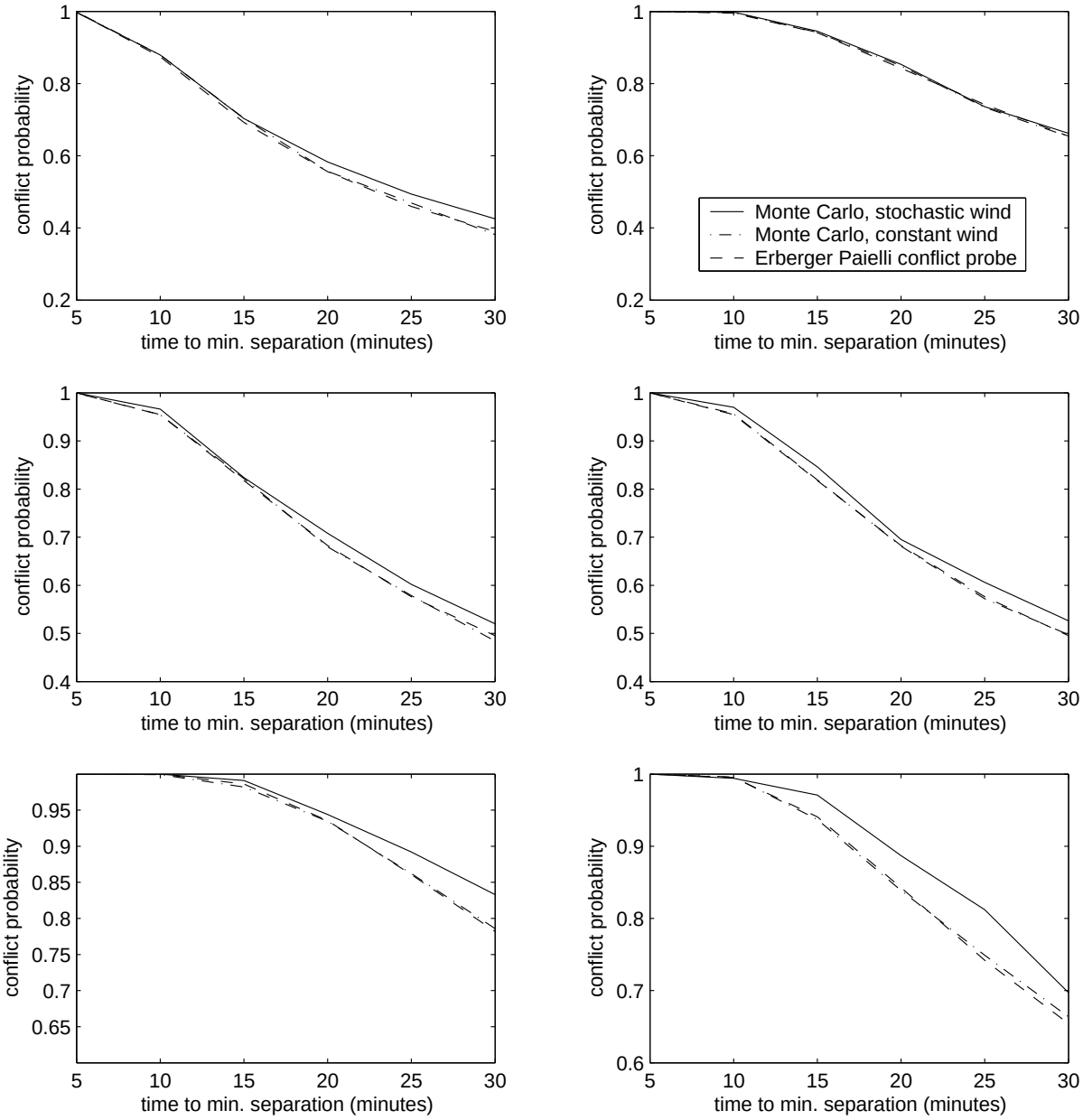

Figure 5: Conflict probability for different crossing angles. The right hand figure shows the results of simulations with both aircraft in the same wind field. The left hand figure shows aircraft with independent wind fields. The top two figures cover the 45 degree situations, the middle ones 90 degrees and the bottom 135 degrees.

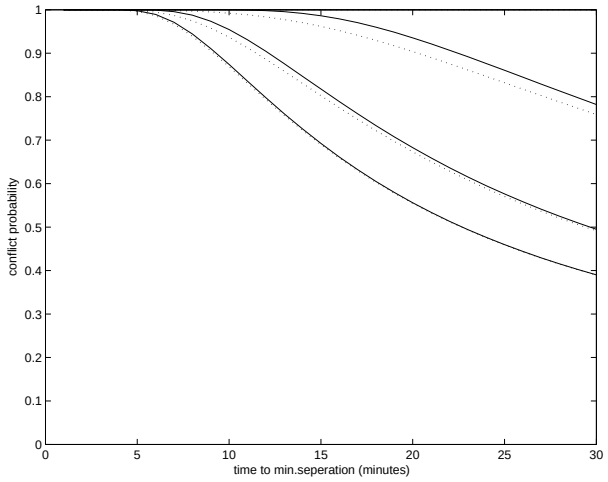

Figure 6: Comparison of conflict probability with (solid line) and without (dotted line) lateral deviation for various crossing angles (45°, 90°, 135°) and zero nominal minimum separation.

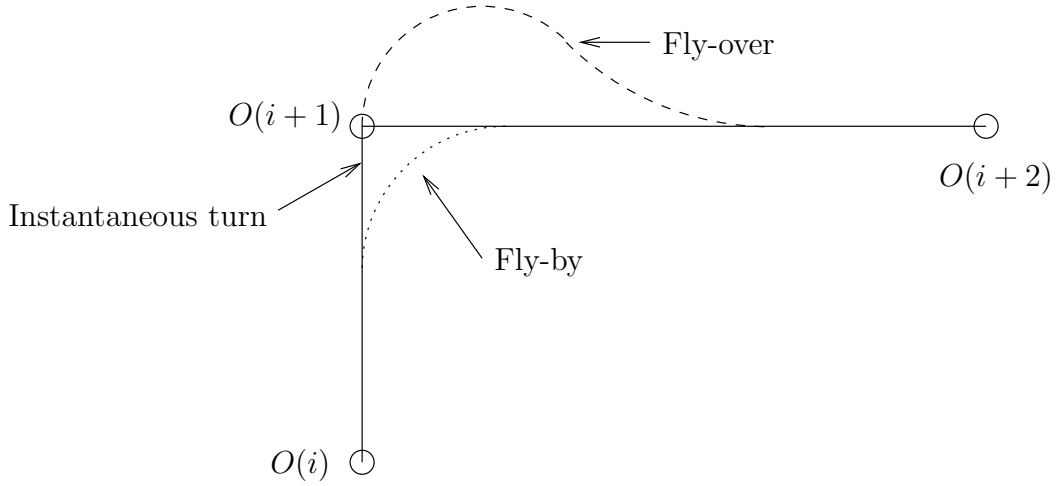

Figure 7: Diagram showing three different types of turn: instantaneous turn, fly-by turn and fly-over turn.

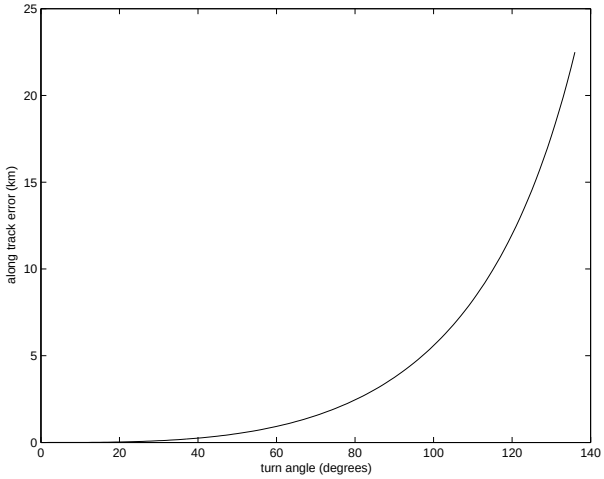

Figure 8: Graph showing the along track error introduced by assuming turns are instantaneous.

3.3 Ignoring the lateral motion altogether

Erzberger Paielli statistics suggest fairly large lateral deviation variances [12]. This is probably caused by aircraft which are not equipped with FMS. Modern FMS equipped aircraft can achieve a cross track deviation of 0.39 NM [2] and modern GPS position sensors can achieve an accuracy of less than 0.02NM which is less than 40m.

Figure 6 suggests that ignoring lateral motion will make a large difference for the short term but not much difference in the long term.

3.4 Decoupling the error model from the aircraft model

This means running the simulation without stochastic effects and then using a separate error model for determining probability of conflict or other risk measures. This is the approach adopted by [13] and [14].

4 Stochastic models used for conflict detection and resolution

4.1 The model of Erzberger and Paielli

This model uses a high quality model for the nominal behavior which includes a realistic turn model and also models accurately climbing and descending [13, 14, 12]. They consider the errors in along track position and across track position to be determined by a Gaussian distribution, with zero mean and variances that grow as a of function time. To calculate the probability of conflict they assume that the errors are constant throughout the aircraft trajectories and they consider the point of minimum separation in the nominal trajectory to find the magnitude of the along track and cross track errors. This will only be accurate if for the period of conflict the aircraft are both travelling on straight paths.

This method has the advantage of having a closed form solution and accurate nominal trajectories. The approximation will generally be good but may produce misleading results for small crossing angles, and for conflict between climbing/descending aircraft.

Correlation between aircraft is not considered but it is possible to extend this method to include correlation for straight and level flight and it may be possible to extend it to non-level flight as well.

4.2 The model of Watkins, Prandini, Lygeros

Introduced by M. Prandini, J. Lygeros in [15] as an evaluation model for conflict detection. It is used in HYBRIDGE by O. Watkins for particle system based Conflict Detection [17]. It is a stochastic differential equation with time varying noise coefficients to mimic Erzberger-Paielli statistics. The stochastic disturbance in this model enters at the velocity level. This model includes waypoints but considers turns to be instantaneous. Only level flight is considered. This model considers lateral guidance in the form of a feedback term for across track error in the stochastic differential equation.

This model will have the same distribution as in Section 4.1 for position but will have a considerably different distribution for velocity.

4.3 The models of Bakker and Blom

These models are used for calculating the incrossing probability which is an approximation for the probability of collision between two aircraft [5, 3, 4]. Various models are proposed for a variety of different situations. In all cases the evolution of each aircraft is a stochastic differential equation with Wiener process entering at the velocity level. This is similar to

the model from Section 4.2 but with the stochastic disturbance acting at the acceleration level instead of the velocity level. In addition an accurate turn model is included.

The solution to the stochastic differential equation is calculated either analytically or through Monte Carlo simulation. The resulting distributions for position and velocity are used to calculate the incrossing proability.

4.4 The model of Hu and Prandini

This model was introduced in [**?**]. The model was developed in HYBRIDGE. This model considers uses a stochastic differential equation where the disturbance acts at the velocity level as in Section 4.2 but in this case the disturbance is spatially correlated to model the effect of the wind being spatially correlated. This model includes turns which are modelled as being instantaneous changes in direction which occur at fixed times.

4.5 Other probabilistic models

This section has concentrated on models that are in use within HYBRIDGE. For an overview of other models used in conflict detection and resolution see [10].

Model	Wind correlation	lateral guidance	Turns	Variables
Hu and Prandini	Spatial, zero temporal	None	Instant	Spatial position
Watkins, Prandini and Lygeros	None	yes	Instant	Spatial position, heading
Erzberger and Paielli	Zero spatial, perturbations considered to be constant near point of minimum separation.	Nominal only	Accurate	Along track distance, velocity, altitude.
D1.3 Model	Spatial and Temporal	Yes	Accurate	Spatial position, heading, velocity
Bakker and Blom	Temporal correlation, Spatial correlation is one at small distances and zero elsewhere.	Yes	Accurate	Spatial position, velocity, and more.

Table 4: Comparison of simplifications made in each reduced model.

5 Concluding Remarks

In this report we have discussed a number of improvements to the model presented in [7] and also a number of simplifications that can be made to the model so that it can be used for Monte Carlo conflict detection and resolution, without significant loss in its ability to predict dangerous encounters. As this is the end of WP1 the next step is to integrate the model with the Monte Carlo methods being developed in WP5.

References

[1] Phare : Efms phase 1b. Technical Report DOC 96-70-15, EUROCONTROL, July 1996.

[2] Navigational accuracy of aircraft equpped with advanced navigation systems. Technical Report EEC Report NO. 216, EUROCONTROL, June 1988.

[3] G. Bakker, H. Kremer, and H. Blom. Geometric and probabilistic approaches towards conflict prediction. In 3^{rd} *USA/Europe Air Traffic Management R & D Seminar*, Napoli, Italy, 13-16 June 2000.

[4] G.J. Bakker, H.J. Kremer, and H.A.P. Blom. Probabilistic approaches towards conflict prediction. In G.L. Donohue and A.G. Zellweger, editors, *Air Transportation systems engineering*, pages 677–694. AIAA, 2001.

[5] H.A.P. Blom and G.J. Bakker. Conflict probability and incrossing probability in air traffic management. In *Proc. IEEE Conf. on Decision and Control*, pages 2421–2426, 2002.

[6] Eurocontrol Experimental Centre. User manual for the base of aircraft data (BADA) revision 3.3, 2002.

[7] W. Glover and J Lygeros. A multi-aircraft model for conflict detection and resolution algorithm validation. Technical Report WP1, Deliverable D1.3, HYBRIDGE, July 23, 2003.

[8] Steven M. Green, Michael P. Grace, and David H. Williams. Flight test results: CTAS and FMS cruise/descent trajectory prediction accuracy. In *3rd USA/EUROPE Air Traffic Management R&D Seminar Napoli, Italy*, June 2000.

[9] Jianghai Hu, Maria Prandini, and Shankar Sastry. Aircraft conflict detection in presence of spatially correlated wind perturbations. In *AIAA Guidance, Navigation and Control Conference*, August 2003.

[10] James K. Kuchar and Lee C. Yang. A review of conflict detection and resolution methods. *IEEE Transactions on Intelligent Transportation Systems*, 1(4):179–189, 2000.

[11] Stephane Mondoli and Dianna Liang. Improving trajectory forecasting through adaptive filtering techniques. In *Proc. 5th USA/Europe ATM R&D Seminar*, June, 2003.

[12] R. A. Paielli. Empircal test of conflict probability estimation. Technical report, NASA Ames Research Center, Moffett Field, CA 94035-1000, U.S.A., 1998.

[13] R. A. Paielli and H. Erzberger. Conflict probability estimation for free flight. Technical report, NASA Ames Research Center, Moffett Field, CA 94035-1000, U.S.A., 1997.

[14] R. A. Paielli and H. Erzberger. Conflict probability estimation generalized to non-level flight. Technical report, NASA Ames Research Center, Moffett Field, CA 94035-1000, U.S.A., 1999.

[15] M. Prandini, J. Hu, J. Lygeros, and S. Sastry. A probabilistic approach to aircraft conflict detection. *IEEE Transactions on Intelligent Transportation Systems*, 1(4), 2000.

[16] R.E.Cole, C. Richard, S. Kim, and D. Bailey. An assessment of the 60 km rapid update cycle (ruc) with near real-time aircraft reports. Technical Report NASA/A-1, MIT Lincoln Laboratory, July 15, 1998.

[17] Oliver Watkins and John Lygeros. Stochastic reachability for discrete time systems: An application to aircraft collision. In *42nd IEEE Conference on Decision and Control*, September 2003.